Materials Research. 2025; 28(suppl. 1): e20250053
DOI: https://doi.org/10.1590/1980-5373-MR-2025-0053

Use of Ceramic Material and Granite to Increase the Thermal Efficiency of the Solar Stills

Vanessa Rosales Conserva[a], *Kênia Kelly Freitas Sarmento*[a], *Camylla Barbosa Silva*[a], *Karyna Steffane da Silva*[a], *Keila Machado de Medeiros*[b], *Carlos Antônio Pereira de Lima*[a*]

[a]*Universidade Estadual da Paraíba, Campina Grande, PB, Brasil.*
[b]*Universidade Federal do Recôncavo da Bahia, Feira de Santana, BA, Brasil.*

Received: January 9, 2025; Revised: May 2, 2025; Accepted: May 17, 2025

The increase in population has intensified the demand for water resources, leading to scarcity due to constraints in their availability, extraction, and sustainable utilization across various regions of the world. This study aimed to evaluate the performance of asymmetric pyramid-shaped solar stills units enhanced with photothermal materials to improve distilled water yield. Three identical solar still systems were constructed, with sensible heat storage materials incorporated into the trays of two of the units. In the first solar still unit (SS1), ceramic tiles were used as the heat storage medium; in the second (SS2), granite was employed; and in the third (SS3), no additional material was introduced. The corresponding distilled water outputs were 2424.80 $mL.m^{-2}$ for SS1, 2992.00 $mL.m^{-2}$ for SS2, and 2121.00 $mL.m^{-2}$ for SS3. The incorporation of granite and ceramic tiles in the solar still units led to efficiency increases of 23% and 7%, respectively, compared to the reference system. Following the solar still process, significant reductions were observed in physicochemical parameters, particularly sodium, which decreased by 97%, 96%, and 96% in SS1, SS2, and SS3, respectively. All remaining parameters were also reduced and remained within acceptable potable water standards.

Keywords: *Solar distillation, potability, photothermal materials, heat sensitive, brackish water.*

1. Introduction

Drought is one of the most devastating natural disasters in the world and can occur in all climate zones[1]. However, as noted by Hammoodi et al.[2], this issue can be mitigated through the use of high-capacity water distillation systems. Nevertheless, the operation of such equipment typically relies heavily on fossil fuels, resulting in significant environmental impacts. Consequently, distillation technologies powered by renewable energy sources, particularly solar energy, are strongly recommended due to their economic viability and reduced environmental footprint.

In the context of increasing water scarcity, solar still has emerged as a highly effective and indispensable technology for addressing this challenge[3]. Solar distillation is a physical separation process aimed at removing excess dissolved salts from water, producing low-salinity water suitable for a variety of uses[4]. A solar still unit is a system designed to convert saline or brackish water into potable water by harnessing solar energy as the primary power source[5].

Solar still systems are considered reliable due to their simplicity, low cost, ease of maintenance, and minimal environmental impact. However, their relatively low efficiency and limited productivity remain significant challenges that need to be addressed[6]. The pyramid-type solar still unit features an increased evaporation surface relative to the basin area, enhancing its thermal performance. Ongoing research efforts focus on the integration of additional components to improve system efficiency and, consequently, increase freshwater yield[7].

The use of photothermal materials for thermal energy storage has been widely recognized as an environmentally sustainable approach for producing clean water from saline sources. In recent years, significant research efforts have focused on enhancing solar-to-thermal energy conversion efficiency to improve the overall performance of solar still systems[8]. Another emerging technology is photothermal membrane distillation (PMD), which generates water vapor from thin-film surfaces. In this process, solar radiation is absorbed and converted into localized heat, thereby minimizing thermal losses and enhancing the efficiency of solar-to-thermal energy conversion[9]. The integration of photothermal materials in solar still systems has garnered significant interest due to their positive impact on thermal management and key operational parameters, ultimately enhancing overall system efficiency. This improvement stems from their superior sunlight absorption capabilities and high efficiency in converting solar radiation into thermal energy[10].

Photothermal materials can be classified based on their thermal energy storage mechanisms into three categories: sensible heat, latent heat, and thermochemical heat storage[11]. Although sensible heat storage materials exhibit lower energy density compared to the other types, they are the most extensively developed and widely used due to their simplicity and cost-effectiveness[12]. The incorporation of thermal energy storage materials in solar distillers enhances

*e-mail: caplima@servidor.uepb.edu.br
Associate Editor: Eliana Muccillo.
Editor-in-Chief: Luiz Antonio Pessan.

system efficiency and, consequently, water productivity by minimizing heat losses within the distillation unit[13].

Owing to their thermal stability, favorable heat transfer properties, and low cost, Sensible Heat Storage (SHS) materials are widely utilized in both high- and low-temperature applications. These materials may originate from natural sources or be synthetically manufactured[14]. SHS materials are primarily classified into solid-state and liquid-state categories, which are further subdivided into natural and manufactured thermal energy storage materials[11]. Figure 1 illustrates the classification scheme for sensible heat storage materials.

Several studies have explored the integration of photothermal materials in solar still systems; however, experimental investigations specifically employing granite and ceramic tiles as thermal storage media remain scarce. Mevada et al.[15] conducted a comparative study on a basin-type solar still system incorporating various photothermal materials. Their findings indicated that the use of such materials led to increased temperatures in both the glass cover and the basin, resulting in a 76% improvement in daily water yield compared to a conventional solar still unit. Similarly, Selvaraj and Natarajan[16] investigated the use of black glass spheres as a thermal energy storage material in a double-slope basin-type solar still system.

Attia et al.[17] employed black gravel of varying particle sizes to enhance the heat transfer rate in a solar still system, aiming to improve its overall efficiency. The study tested four gravel sizes (4, 8, 11, and 16 mm) and compared the performance of the modified system against a control unit operating under identical climatic conditions but without the addition of gravel. The results showed that the highest cumulative water productivity was achieved with the solar still unit containing 16 mm gravel. Li et al.[18] employed polydimethylsiloxane/carbon nanotube (PDMS/CNT) composites in modified solar still systems to enhance operational efficiency.

Zhang et al.[19] developed a vinylidene fluoride-based photothermal membrane coated with ferric tannate and encapsulated with titanium dioxide. The material demonstrated high efficiency and reusability under simulated solar irradiation, exhibiting effective photothermal conversion, excellent fluid transport, and stability in aqueous environments, highlighting its potential for water distillation applications. Rajan et al.[20] investigated methods to enhance the performance of pyramid-type solar still units through the incorporation of sensible heat storage materials (such as metal parts, stones, and shells), latent heat storage billets (including water and wax), and evaporative surface materials (wick and sponge). The study reported that the use of sensible and solid thermal storage materials increased productivity by 84% compared to a conventional distiller. Latent heat storage materials in billet form improved productivity by 69%, while evaporative surface modifications expanded the exposure area and led to a 61% increase in water yield relative to the unmodified system.

Considering the foregoing, the present study aims to evaluate the efficiency of employing photothermal materials for sensible heat storage in asymmetric pyramid-type solar stills systems, with the objective of increasing distilled water production. While previous studies have investigated the use of materials for sensible heat storage, the innovation of this research lies in the application of granite and ceramic tiles within an asymmetric pyramid configuration. These materials were selected for their favorable thermophysical properties, low cost, wide availability, and ease of acquisition. The use of such photothermal materials is therefore justified as a strategy to enhance the thermal performance and productivity of solar stills systems. Furthermore, the implementation of this technology may offer substantial benefits to remote or underserved communities exposed to high levels of solar radiation and facing challenges in water availability, as sustainable water supply solutions play a crucial role in improving quality of life and promoting social well-being.

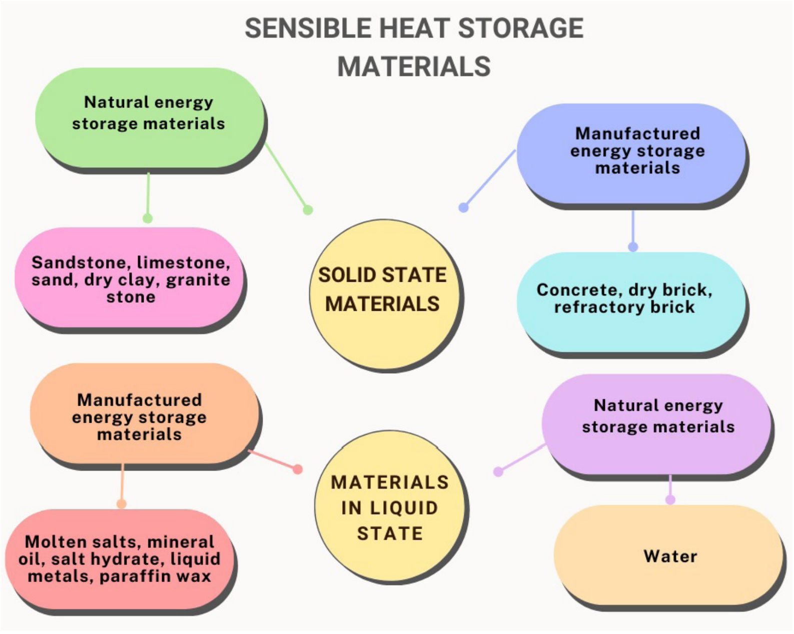

Figure 1. Classification of sensible heat storage materials. Prepared by the author, 2024.

2. Materials and Methods

The project was carried out at the Center for Science and Technology of the State University of Paraiba, Brazil, located at a latitude of 7º13'11" S and a longitude of 35º52'31" W, with an average elevation of approximately 550 meters above sea level. An asymmetric pyramid-shaped solar still model was selected, as illustrated in Figure 2a the conventional pyramid configuration and (b) the pyramid configuration incorporating sensible heat storage materials and Figure 3 presents the schematic diagram of the solar still.

2.1. Photothermal materials

Based on a literature review of photothermal materials, sensible heat storage (SHS) was selected for investigation. This selection was primarily motivated by the material's accessibility, low cost, and operational simplicity. Taking into account criteria such as thermophysical properties, availability, and cost, the following materials were selected for analysis: gravel, granite, ceramic tiles, iron, and glass spheres (as detailed in Table 1).

Red ceramic tiles are manufactured from common clay, with their properties being influenced by both the raw material

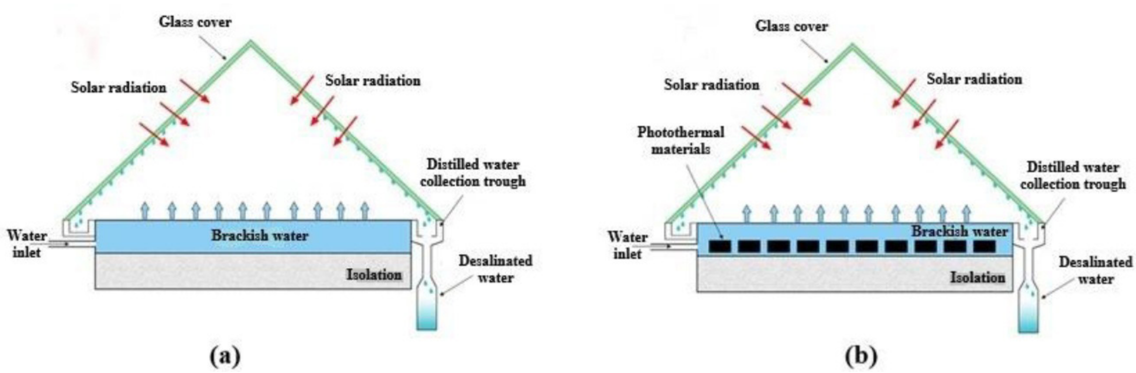

Figure 2. Schematic drawing of the solar still: (a) conventional pyramid type and (b) pyramid type using sensible heat storage materials. Prepared by the author, 2024.

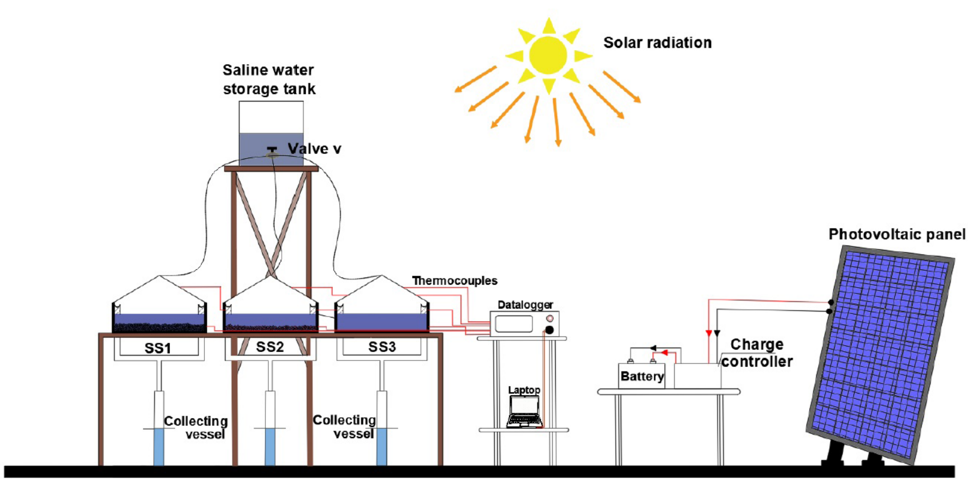

Figure 3. Schematic drawing of the solar still. Prepared by the author, 2024.

Table 1. Thermophysical properties of photothermal materials under investigation. Adapted from[10,19,20].

Material	Density (kg.m^{-3})	Specific heat (kJ.kg^{-1}.K^{-1})	Thermal conductivity (W.m^{-1}.K^{-1})	Thermal diffusivity (m^2.s^{-1})	Volumetric heat capacity (kJ.m^{-3}.K^{-1})
Gravel[19]	2400	1.0	1.8	0.75 x10^{-6}	2400
Granite[10]	2640	0.82	1.7 – 4.0	1.84 x10^{-6}	2164
Tile[10]	1400	0.80	0.9 – 1.2	0.52x 10^{-6}	1120
Iron[20]	7200	0.56	37.0	22.8 x 10^{-6}	3571
Glass[20]	2710	0.80	0.7 – 0.9	0.3 x 10^{-6}	2168

composition and the production process. These tiles typically exhibit a high-water affinity, resulting in greater absorption rates compared to natural stones[21]. Glass is a transparent surface that generally allows a high heat flow due to its ability to directly transmit incident solar radiation to the interior, increasing the internal temperature and promoting the greenhouse effect. Because it is transparent, glass absorbs short-wave radiation and consequently has a high transmittance index[22].

Gravel, granite, ceramic tiles, iron, and glass spheres were placed in separate trays, each containing identical volumes of water and material, as illustrated in Figure 4. These trays were exposed to solar radiation from 9:00 a.m. to 2:00 p.m., corresponding to the period of highest solar irradiance. The experiment was subsequently repeated using the same basins and materials coated with black paint, aiming to enhance heat absorption by increasing surface absorptivity.

To monitor the temperatures of the materials, the Integrated Multianalysis System[23] was employed, enabling temperature recordings at 30-minute intervals throughout the specified time range. A thermal analysis of the photothermal materials was conducted to support the selection of the two materials exhibiting the highest thermal efficiency.

2.2. Productivity and efficiency of solar still

The efficiency of solar still systems can be assessed on both hourly and daily bases. Hourly efficiency is defined as the ratio between the average latent heat associated with the volume of water produced per hour and the amount of solar energy absorbed during that same period. As a result, variations in solar irradiation throughout the day lead to corresponding fluctuations in hourly solar energy efficiency [24]. Both hourly and daily efficiencies were calculated using Equations 1 and 2, respectively[25]:

$$\eta_h = \frac{\left(M_w x \lambda_w\right)/3600}{\left(A_b x I\right)} \tag{1}$$

$$\eta_D = \frac{1}{n}\sum_n \eta_h \tag{2}$$

where M_w is the hourly water production (kg), A_b is the area of the basin (m^2), n is the duration of the experiment in hours, I is the solar irradiation (W.m^{-2}) and λ_w is the latent heat of vaporization of water (J.kg^{-1}), which is calculated as a function of water temperature, as shown in Equation 3:

$$\lambda_w = \begin{pmatrix} 2501{,}9 - 2{,}40706T_w + 1{,}192217 \cdot 10^{-3} \cdot \\ T_w^2 - 1{,}5863 \cdot 10^{-5} \cdot T_w^3 \end{pmatrix} \cdot 10^3 \tag{3}$$

The volume of water produced by solar still systems varies according to the design configuration, solar radiation levels, and prevailing weather conditions[26]. The hourly productivity of distilled water is determined using Equation 4[27].

$$m = h_{ev}\frac{Ac}{As}\cdot\left[\frac{T_w - T_g}{\lambda_w}\right].3600 \tag{4}$$

where m is the water production (L.m^{-2}.dia^{-1}), λ_w is the latent heat of water vapor (J.kg^{-1}).

The mass of distilled water is calculated using the equation proposed by Dunkle[28], using the measured values of water temperature, glass cover temperature, and tray temperature, the physical parameters were fixed and not sourced from external references. During the experimental period, the solar still units were operated simultaneously under identical environmental conditions. This setup enabled the collection of data related to estimated daily distillate production, water temperature, and glass temperature, thereby allowing a comprehensive evaluation of the effectiveness and efficiency of the proposed system modifications.

2.3 Experimental model setup

Three identical solar stills units were constructed, each designed to meet the operational requirements of the proposed technology. The design prioritized ease of operation, minimized thermal losses, corrosion resistance, and enhanced durability. The units were designated as SS1, SS2, and SS3, as illustrated in Figure 5.

Figure 4. Temperature check of materials used. Prepared by the author, 2024.

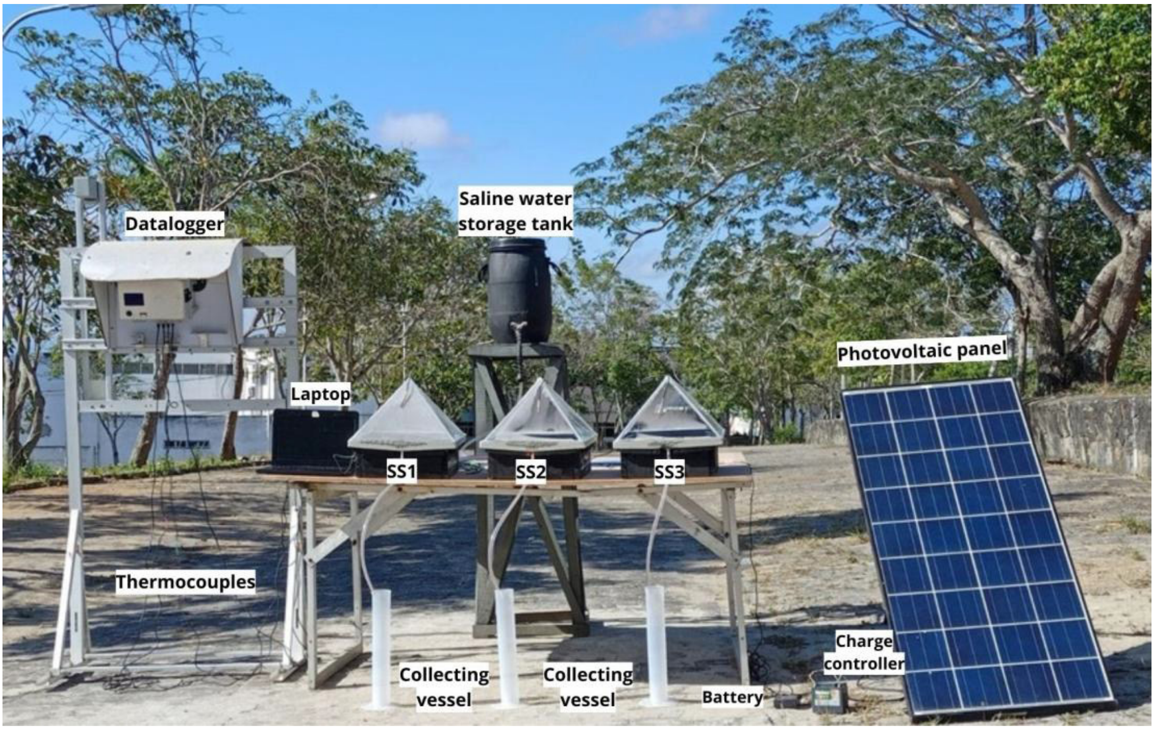

Figura 5. Experimental solar still system. Prepared by the author, 2024.

Each solar still unit consists of three main components: a thermal insulation system, a glass cover for condensate collection, and an aluminum tray. The solar still measure 0.50 m in length, 0.40 m in width, with a total effective area of 0.20 m^2. The aluminum trays are rectangular, measuring 0.44 m in length, 0.30 m in width, and 3 mm in thickness, and were painted black to enhance solar radiation absorption. The photothermal materials were placed on the tray surfaces, as illustrated in Figure 4. Subsequently, 4 mm-thick glass covers were installed at a 48° inclination to the horizontal plane. These covers were hermetically sealed to prevent vapor leakage and to intensify the greenhouse effect within the system.

The solar still units were operated from 07:00 to 17:00, positioned in an open, unobstructed area to ensure maximum solar exposure. Multiple experimental trials were conducted, maintaining a constant water depth of 1 cm in each unit. All solar stills systems were operated simultaneously under identical environmental conditions to ensure the reliability and comparability of the results.

Solar radiation was measured in the range between 1.0 to 1,300.0 $W.m^{-2}$ with an accuracy of ± 1.0 $W.m^{-2}$. Temperatures at different points of the system were measured using K-type thermocouples, with a measurement range of -50 to 300 °C and an accuracy of ± 1.0 °C. All readings were stored in a data acquisition system. The datalogger used for monitoring the solar stills units was developed by[23]. The system was also employed to measure meteorological parameters, including solar radiation and ambient temperature, through a photovoltaic panel-based setup. Additionally, it recorded the water and glass cover temperatures of the solar stills, as illustrated in Figure 6.

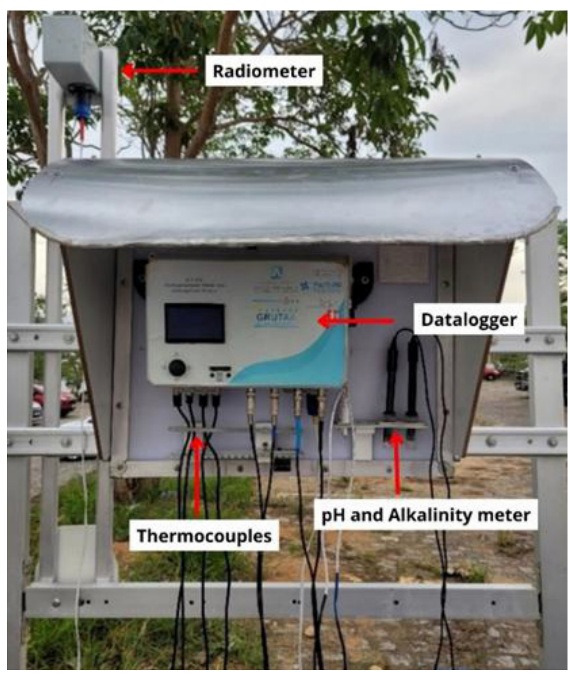

Figura 6. Integrated Multianalysis System for measuring operational parameters. Prepared by the author, 2024.

The volume of distilled water produced was measured using a graduated cylinder (0 a 1000 mL) with an accuracy of ± 10.0 mL. Standard accuracies and uncertainties of measuring instruments are shown in Table 2, were calculated for thermocouples, radiometer, and graduated cylinder.

In the experiments, the uncertainties were classified as Type B, as they are associated with systematic errors and were determined based on external sources, such as calibration certificates and manufacturer specifications. Accordingly, the uncertainty analysis for each measuring instrument was performed using Equation 5[29], where u represents the estimated uncertainty and a denotes the standard accuracy of the instrument.

$$u = \frac{a}{\sqrt{3}} \tag{5}$$

Water is considered unsuitable for use when its quality parameters exceed the limits established for a specific purpose[30]. To evaluate the potability of the water before and after the experiments, physicochemical analyses were conducted on both brackish and desalinated water samples, following the procedures outlined in the *Standard Methods for the Examination of Water and Wastewater*[31]. As shown in Table 3, the selected parameters are key indicators of water salinity.

3. Results and Discution

To determine the most suitable photothermal material for integration into the solar still systems, preliminary tests were conducted using gravel, granite, ceramic tiles, iron, and glass spheres. These materials were placed in multiple trays containing identical volumes of both water and material, as illustrated in Figure 4.

Figure 7 presents a comparative analysis of the hourly temperature variations for different photothermal materials, gravel, glass spheres, iron, granite, and ceramic tiles, along with solar radiation. The test commenced at 9:00 a.m., with maximum temperatures recorded at 12:00 p.m. as follows: water (29.00 °C), gravel (37.12 °C), glass spheres (36.81 °C), iron (37.10 °C), granite (38.50 °C), and tiles (38.91 °C). The results demonstrate a clear temperature increase across all photothermal materials, with respective increases of 8.1 °C (gravel), 7.8 °C (glass spheres), 8.1 °C (iron), 9.5 °C (granite), and 9.9 °C (tiles), when compared to the temperature of water alone. These peak temperatures coincided with the highest recorded solar irradiance of 1009 $W \cdot m^{-2}$.

As illustrated in Figure 7, all tested materials contributed to an increase in water temperature within the trays. Among them, granite and ceramic tile exhibited the highest volumetric heat capacity values. According to Patel and Kumar[32] thermal conductivity refers to a material's ability to conduct heat, while volumetric heat capacity indicates its capacity to store thermal energy. Gravel and granite are distinct types of rock materials that offer several advantages, including low cost, wide availability, non-toxicity, and non-flammability[12]. These characteristics make them excellent candidates for use as heat storage media in solar stills systems.

Priya and Mahadi[33] investigated the effect of applying black paint in solar stills systems and observed a 35% increase in water production, confirming that the use of black paint enhances heat transfer. Based on the temperature profile results of the photothermal materials inside the solar still unit, granite and ceramic tile were selected for the present study, as both exhibited consistently higher temperatures throughout the experimental period.

3.1. Analysis of the initial performance of solar stills

An initial performance analysis of the solar still system was conducted to evaluate its operational efficiency under the proposed conditions. Key parameters, including water temperature, photothermal material temperature, incident solar radiation, and distillate yield, were continuously monitored. These indicators enabled the characterization of the thermal behavior of the selected materials and the assessment of the effectiveness of the implemented modifications. The results provided a basis for system validation and informed adjustments aimed at maximizing process efficiency.

The performance of solar still systems is strongly influenced by the internal temperature distribution. In particular, the temperature gradient between the water

Table 2. Accuracy and standard uncertainty for measuring instruments.

Instrument	Range	Accuracy	Standard uncertainty
Radiometer	1 to 1300 $W.m^{-2}$	± 10 $W.m^{-2}$	2.5%
Digital thermocouple	-50 to 300 °C	± 0.1 °C	0.05 °C
Graduated cylinder	0 to 1000 mL	± 10 mL	0.05 mL

Table 3. Physical-chemical parameters used.

Physico-chemical properties	Unity
pH	–
Electric conductivity	$\mu S \cdot cm^{-1}$
Total hardness as $CaCO_3$	$mg \cdot L^{-1}$
Total alkalinity as $CaCO_3$	$mg \cdot L^{-1}$
Sodium as Na^+	$mg \cdot L^{-1}$
Chlorides as Cl^-	$mg \cdot L^{-1}$
Turbidity	NTU

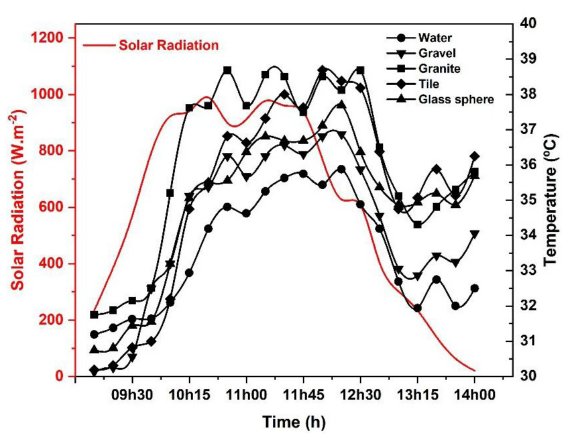

Figure 7. Temperature profile of photothermal materials. Prepared by the author, 2024.

surface and the glass cover plays a critical role in enhancing evaporation and condensation processes, thereby improving system efficiency. Figure 8 presents the results of a new experimental run, illustrating the dynamic variation of water temperature, glass cover temperature, ambient temperature, and solar radiation for solar still units SS1, SS2, and SS3, operated simultaneously. SS1 incorporated ceramic tiles, SS2 employed granite as the photothermal material, while SS3 served as the control unit without any heat storage material.

All monitored temperatures reached their peak values at 12:30 p.m., approximately two and a half hours after the maximum recorded solar radiation of 1039.0 W·m^{-2}. At this time, the water temperature reached 62 °C in SS1, 63 °C in SS2, and 57 °C in SS3. It was observed that the temperature profiles closely followed the fluctuations in solar radiation. Variations in irradiance were primarily attributed to climatic conditions, particularly cloud cover. Notably, between 12:30 and 13:00, a period during which peak solar radiation is typically expected, the experiment recorded unusually low irradiance values due to transient cloud shading. Similar trends were reported by Cardoso et al.[26]. Between 15:30 and 17:00, the water temperatures in solar stills units SS1 and SS2 were 41 °C and 39 °C, respectively, at 15:30, indicating enhanced thermal retention within the trays. This resulted in a slower temperature decline compared to SS3, which registered 37 °C at the same time. These results confirm that the incorporation of photothermal materials in solar stills units enhanced both the temperature elevation and thermal retention capacity of the system.

3.2. *Temperature and water productivity profile of solar stills*

Several factors can influence the productivity of solar stills systems. Design parameters such as the inclination angle of the condensing glass cover, the water depth, the tray surface area, and the effectiveness of thermal insulation can be optimized to enhance system performance. However, meteorological variables such as solar radiation intensity, wind speed, and ambient temperature are uncontrollable and represent external factors that significantly affect desalination efficiency.

Figure 9 presents the temperature profiles of the solar stills alongside the cumulative water productivity. It is evident that the distillate production follows the temperature variations of the water and glass cover, as observed at 12:30 p.m., when the glass temperature in SS1 reached 48 °C and the hourly distillate yield peaked at 333.3 mL.m^{-2}. This contributed to a cumulative daily production of 2,424 mL.m^{-2}.day^{-1}. In SS2, it is observed that distillate production closely follows the variation in glass temperature. At 12:30 p.m., the glass temperature reached 45 °C, and the subsequent measurement recorded the highest water yield, with a production of 340.9 mL.m^{-2}. SS2 achieved a daily desalinated water production of 2,992 mL.m^{-2}.day^{-1}. These results are consistent with the findings of Attia et al.[17], who investigated the effect of gravel in solar stills systems and reported a maximum daily yield of 4,900 mL.m^{-2}.day^{-1}.

The highest hourly production of desalinated water from SS3 was 250.0 mL.m^{-2}, which occurred after a considerable increase in solar radiation intensity, when the glass temperature reached 45 °C. The accumulated water production at the end of the experiment was 2,121 mL.m^{-2}.day^{-1}. The solar stills using photothermal materials not only reached their peak desalinated water production faster than SS3 but also achieved a higher total water yield.

Conserva et al.[34] studied the experimental performance of two asymmetric pyramid-type solar stills: a hybrid solar still (SSH) and a passive solar still (SSP). The passive solar still (SSP) achieved a daily water productivity of 4,794 L.m^{-2}.day^{-1}. Khechekhouche et al.[35] reported a maximum hourly water production of 640 mL.m^{-2} using a zinc plate in a single-slope type solar still.

3.3. *Production of desalinated water according to solar radiation*

Figure 10 shows the water production as a function of solar radiation in solar stills SS1, SS2, and SS3. It can be observed that SS2 achieved higher water production compared to the other two systems, SS1 and SS3. Specific mass and specific heat are key properties commonly used

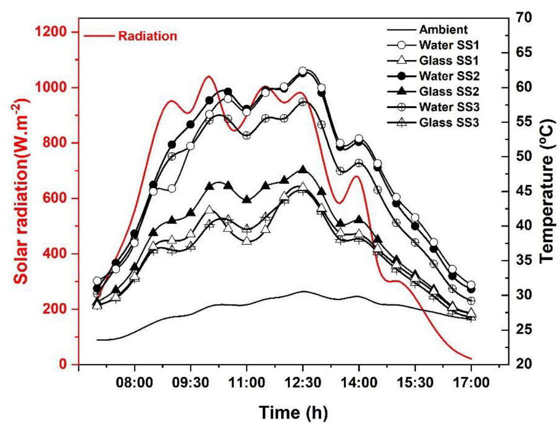

Figure 8. Temperature profiles and incidence of solar radiation SS1, SS2 and SS3. Prepared by the author, 2024.

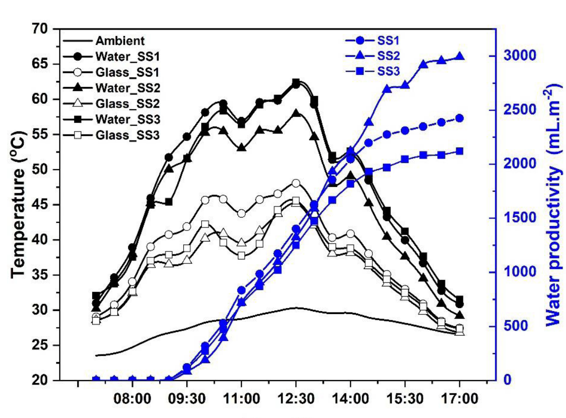

Figura 9. Desalinated water production for SS1, SS2 and SS3. Prepared by the author, 2024.

in thermodynamic analysis. The product of these two properties is referred to as the volumetric heat capacity, which represents a material's ability to store thermal energy[36]. The enhanced productivity observed in SS2 can be attributed to the incorporation of photothermal material in the solar still basin, specifically granite, which possesses a higher thermal storage capacity compared to tile, as indicated in Table 1. Furthermore, the application of black paint improved the thermophysical performance of the materials, with granite exhibiting more favorable properties than tile. Ravichandran et al.[37] studied the application of granite as a sensible heat storage material in solar still systems and concluded that its use resulted in a 29% increase in the overall productivity of the solar still.

Throughout the experiment, variations in solar radiation intensity resulted in changes in water and glass temperatures, which directly impacted the productivity of the solar stills. The selection of a 1 cm water layer in the basin enhanced the system's performance, as thinner water layers facilitate faster heating, promoting quicker evaporation and subsequent condensation of the distillate due to the reduced thermal mass. Panchal and Sathyamurthy[5] state that the convective heat transfer coefficient between the inner glass cover and the water depends significantly on the depth of the water in the basin.

3.4. Thermal efficiency of solar still

Thermal efficiency is an important parameter for evaluating the performance of a solar still. It is influenced by factors such as solar irradiance, ambient temperature, wind speed, and relative humidity[38]. Figure 11 presents the variation in the hourly efficiency of SS1, SS2, and SS3 as a function of operating time and solar radiation. Higher efficiency values were observed during periods of decreasing solar irradiance, which can be attributed to the thermal energy accumulated in the water, due to its high specific heat capacity. This property enables water to act as an effective absorber and reservoir of thermal energy. Furthermore, the construction of the solar stills prioritized effective thermal insulation, reducing heat losses and contributing to the maintenance of elevated internal temperatures even under lower solar irradiance.

It can be observed that the hourly efficiencies obtained generally follow the solar radiation trend, indicating that the efficiency of the solar stills is directly proportional to solar irradiance. However, from 2:30 p.m. onwards, an unexpected increase in efficiency was recorded for systems SS1, SS2, and SS3, despite the decline in solar radiation. This phenomenon can be attributed to the high thermal capacity of the water and the heat retention of the materials used, which sustained the distillation process even under reduced solar input. Tabrizi et al.[39] also concluded that the thermal capacity of water enables the solar still process to persist, resulting in increased efficiency even during periods of declining solar radiation.

It is also observed that SS2 exhibited the highest daily efficiency, reaching a maximum hourly efficiency of 174%, followed by SS1 with 166% and SS3 with 159%. These results indicate that the use of thermal energy storage materials, such as granite and tile, contributed significantly to improving the performance of the solar stills.

Sensible Heat Storage (SHS) systems offer the advantage of operating at higher temperatures, making them more favorable than Liquid Heat Storage Systems (liquid SHS). It is important to highlight that, in SHS, the storage medium, whether liquid or solid, does not undergo a phase change[40]. Table 4 presents selected studies involving the application of SHS systems.

Gravel and granite are rock materials that exhibit excellent thermal performance, making them suitable for thermal energy storage applications. Solid-state SHS materials, including rocks, metals, concrete, sand, bricks, and pebbles, are widely used in various energy storage applications due to their ability to withstand very high temperatures. These materials have no leakage problems, exhibit high thermal consistency, low investment cost, are easy to implement, and are suitable for various practical applications. In addition, they do not face challenges such as high vapor pressure of water, freezing or boiling, and do not present the disadvantages typically associated with other liquids[48].

3.5. Monitoring the quality of desalinated water

Physicochemical analyses of multiple potability parameters were conducted to evaluate the performance of the solar still system. Based on the results, the solar still process proved

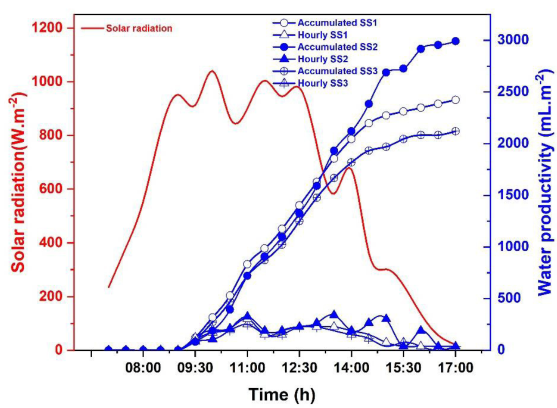

Figure 10. Water productivity solar stills SS1, SS2 and SS3. Prepared by the author, 2024.

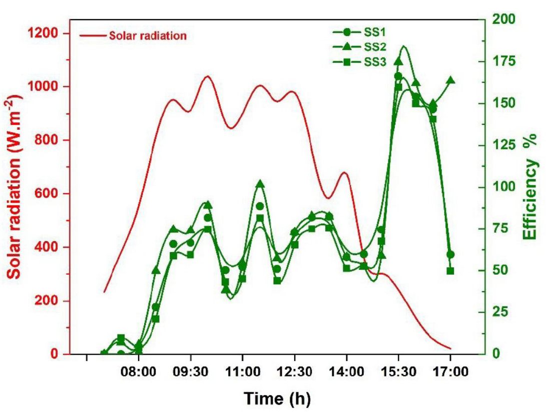

Figure 11. Variation in hourly efficiency for SS1, SS2 and SS3. Prepared by the author, 2024.

Table 4. Application of sensible heat storage (SHS) materials in solar stills.

Authors	Materials SHS	Results
Patel and Kumar[32]	Thermal oil (HP-500)	An increase of 11.24% in solar still productivity was achieved.
Samuel et al.[41]	Sponge	Their results demonstrated a 22.73% increase in water production.
Kabeel et al.[42]	Fabric and sand	This resulted in an 18% increase in water productivity.
Benatiallah et al.[43]	Gravel, sand and polyethylene	Gravel yielded the highest water production (5.00 $L.m^{-2}.day^{-1}$), followed by black polyethylene (4.48 $L.m^{-2}.day^{-1}$) and sand (3.84 $L.m^{-2}.day^{-1}$)
Kabeel et al.[44]	Graphite	The efficiency of the single-basin solar still was improved within a range of 25% to 27%
Balaji et al.[45]	Pebbles, stones, bricks, granite and marble	Solar stills incorporating heat storage materials demonstrate higher efficiency.
Panchal et al.[46]	Sandstone and marble	The use of sandstone and marble as heat storage materials resulted in an increase in solar still efficiency by 30% and 14%, respectively.
Arunkumar et al.[47]	Polyvinyl Alcohol (PVA) sponges, pebbles, spherical clay balls and copper oxide nanocoated absorber plate	The use of sponge, pebbles, spherical clay balls, and absorber plate led to efficiency increases of 32%, 44%, 39%, and 53%, respectively.

effective for treating brackish water, as values for electrical conductivity, chlorides, hardness, turbidity, and sodium remained within the potability limits established[49]. Table 5 presents the average physicochemical parameters of both raw and desalinated water.

The pH of the raw water sample was measured at 8.1. Following the solar still process, a reduction in pH was observed, with values of 5.9 (SS1), 6.0 (SS2) and 5.8 (SS3). Electrical conductivity, which reflects the water's ability to conduct electrical current and is directly influenced by the concentration of dissolved salts, showed a significant reduction. Specifically, a 99% decrease in electrical conductivity was recorded in SS1 and SS2, while SS3 exhibited a 98% reduction, indicating the high effectiveness of the solar still process.

Sodium was another critical parameter that exhibited a substantial reduction following the solar still process. The initial water sample presented a salinity concentration of 200 mg $Na^{+}·L^{-1}$, which was reduced by 97%, 96%, and 96% in SS1, SS2, and SS3, respectively. These findings demonstrate the system's effectiveness in sodium removal. Comparable results were reported by Cardoso et al.[50], who achieved reductions of 99.48% and 99.76% in electrical conductivity and complete (100%) sodium removal.

As shown in Table 5, the raw water exhibited a high concentration of chloride ions, with Cl^{-} levels exceeding the maximum permissible limit of 250 $mg·L^{-1}$ established by regulatory standards. The solar still process resulted in a significant reduction in chloride concentration, achieving removal rates of 97% in SS1, 97% in SS2, and 98% in SS3.

In the hardness analyses, where current legislation sets a maximum allowable limit of 500 mg $CaCO_3·L^{-1}$, the values obtained after the solar still process remained within the acceptable range established by the ordinance. This result is consistent with the results reported by Brito et al.[1]. Regarding alkalinity, a reduction greater than 90% was observed across all solar still units, with SS3 showing the most significant decrease, reaching 96%.

As shown in Table 5, all color measurements for the water samples fall within the maximum permissible value established by legislation, which sets the limit at 15 uH. According to Tosic et al.[51], certain physicochemical parameters of water exhibit higher sensitivity and may show increased concentrations during rainy periods.

Table 5. Result of physical-chemical parameters.

PARAMETERS	Water Brackish	Water distilled SS1	Water distilled SS2	Water distilled SS3	Tolerable levels[49]
pH	8.1	6.5	6.7	6.8	6.5-8.5
Electrical conductivity ($\mu S.cm^{-1}$)	3,809.7	89.7	86.4	107.2	-
Chlorides ($mg.Cl^{-1}.L^{-1}$)	4,036.0	95.4	120.0	43.5	250.0
Hardness (mg $CaCO_3.L^{-1}$)	446.4	50.5	38.3	32.2	300.0
Alkalinity (mg $CaCO_3.L^{-1}$)	432.9	33.9	31.6	17.2	-
Turbidity (uT)	2.6	0.5	0.4	0.4	4.0
Sodium (mg $Na^{+}.L^{-1}$)	200.0	6.8	8.2	7.6	200.0
Color (uH)	8.4	12.4	13.1	13.3	15.0

4. Conclusions

Based on the discussions and the results obtained, the following conclusions can be drawn:

- The performance of the pyramid-type solar still system is influenced by both solar radiation intensity and water depth. The solar stills yielded production rates of 2,424.80 mL·m^{-2} (SS1), 2,992.00 mL·m^{-2} (SS2), and 2,121.00 mL·m^{-2} (SS3), respectively.
- It was observed that SS2 exhibited the highest daily productivity, reaching a peak hourly efficiency of 174%, compared to 166% for SS1 and 159% for SS3. These results indicate that the incorporation of sensible heat storage materials, granite and ceramic tile, contributed to the enhanced thermal performance and overall efficiency of the solar stills.
- One of the key potability parameters that demonstrated a significant reduction was sodium concentration. The experiment was conducted using water with an initial salinity of 200 mg Na^+·L^{-1}. Following the solar still process, sodium levels were reduced by 97%, 96%, and 96% in SS1, SS2, and SS3, respectively, confirming the system's effectiveness in improving water quality.
- With regard to the remaining potability parameters, the results obtained are in compliance with current regulatory standards, supporting the feasibility of the system for both research applications and as an innovative, viable solution for obtaining high-quality water in semi-arid regions.

One of the main limitations of this study is the restricted operating time of the distillers, as the experiments were conducted exclusively during periods of direct solar radiation. This constraint affects the system's productivity by limiting the volume of distilled water generated. Nevertheless, the incorporation of photothermal materials shows promising potential to overcome this limitation by enabling extended operation under lower solar intensity, thereby improving efficiency and increasing daily water yield. Although additional limitations such as shading effects and the challenges associated with large-scale implementation must also be taken into account, the present study offers a robust foundation for future research focused on optimizing solar distillation systems.

For future research, it is suggested to extend the experimental period to 12 hours, including the post-solar radiation phase, in order to evaluate the impact of photothermal materials on maintaining water temperature and distiller productivity in the absence of sunlight. In addition, it is recommended to carry out analyses addressing the ideal water depth, the investigation of new photothermal materials, and the evaluation of the combined use of different materials aiming at process optimization.

6. Acknowledgements

The authors would like to thank the Coordination for the Improvement of Higher Education Personnel (CAPES), the National Council for Scientific and Technological Development (CNPq), the grant #2393/2023-d, Paraiba State Research Support Foundation (FAPESQ) for granting scholarships, and the State University of Paraiba (UEPB) for providing laboratories to carry out this work.

7. References

1. Brito YJV, Cardoso MKB, da Silva KS, Silva CB, de Medeiros KM, de Lima CAP. Experimental study of a tray-type solar desalination plant with double inclination for water purification in the semi-arid region of Paraíba. Ground Water. 2020;34(2):156-65. http://doi.org/10.14295/ras.v34i2.29773.
2. Hammoodi KA, Dhahad HA, Alawee WH, Omara ZM, Essa FA, Abdullah AS. Improving the performance of a pyramid solar still using different wick materials and reflectors in Iraq. Desalination Water Treat. 2023;285:1-10. http://doi.org/10.5004/dwt.2023.29226.
3. Shanmugan S, Hammoodi KA, Eswarlal T, Selvaraju P, Bendoukha S, Barhoumi N, et al. A technical appraisal of solar photovoltaic-integrated single slope single basin solar still for simultaneous energy and water generation. Case Stud Therm Eng. 2024;54:104032. http://doi.org/10.1016/j.csite.2024.104032.
4. Abdullah N, Yusof N, Ismail AF, Lau WJ. Insights into metal-organic frameworks-integrated membranes for desalination process: a review. Desalination. 2021;500:114867. http://doi.org/10.1016/j.desal.2020.114867.
5. Panchal H, Sathyamurthy R. Experimental analysis of single-basin solar still with porous fins. Int J Ambient Energy. 2020;41(5):563-9. http://doi.org/10.1080/01430750.2017.1360206.
6. Hammoodi KA, Dhahad HA, Alawee WH, Omara ZM. A detailed review of the factors impacting pyramid type solar still performance. Alex Eng J. 2023;66:123-54. http://doi.org/10.1016/j.aej.2022.12.006.
7. Hammoodi KA, Dhahad HA, Alawee WH, Omara ZM, Yusaf T. Pyramid solar distillers: a comprehensive review of recent techniques. Results in Eng. 2023;18:101157. http://doi.org/10.1016/j.rineng.2023.101157.
8. Wu X, Chen GY, Owens G, Chu D, Xu H. Photothermal materials: a key platform enabling highly efficient water evaporation driven by solar energy. Mater Today Energy. 2019;12:277-96. http://doi.org/10.1016/j.mtener.2019.02.001.
9. Tian S, Li X, Ren J, Zhou Z, Wang F, Shi K, et al. Emerging heat-localized solar distillation systems: solar interfacial distillation VS photothermal membrane distillation. Desalination. 2024;572:117147. http://doi.org/10.1016/j.desal.2023.117147.
10. Thoai DN, Ta QTH, Truong TT, Van Nam H, Van VG. Review on the recent development and applications of three dimensional (3D) photothermal materials for solar evaporators. J Clean Prod. 2021;293:126122. http://doi.org/10.1016/j.jclepro.2021.126122.
11. Mugi VR, Das P, Balijepalli R, Chandramohan VP. A review of natural energy storage materials used in solar dryers for food drying applications. J Energy Storage. 2022;49:104198. http://doi.org/10.1016/j.est.2022.104198.
12. Jemmal Y, Zari N, Asbik M, Maaroufi M. Experimental characterization and thermal performance comparison of six Moroccan rocks used as filler materials in a packed bed storage system. J Energy Storage. 2020;30:101513. http://doi.org/10.1016/j.est.2020.101513.
13. Sarmento KKF, Silva CB, Benedito DAS, Cavalcante GG, Medeiros KM, Lima CAP. Cascade type solar distiller with the use of photothermic materials applied in the treatment of surface water. Appl Therm Eng. 2024;244:122721. http://doi.org/10.1016/j.applthermaleng.2024.122721.
14. Rajan AS, Raja Marimuthu P. Increasing the productivity of pyramid solar still augmented with biomass heat source and analytical validation using RSM. Desalination Water Treat. 2016;5710(10):4406-19. http://doi.org/10.1080/19443994.2014.995133.
15. Mevada D, Panchal H, Ahmadein M, Zayed ME, Alsaleh NA, Djuansjah J, et al. Investigation and performance analysis of solar still with energy storage materials: an energy-exergy efficiency analysis. Case Stud Therm Eng. 2022;29:101687. http://doi.org/10.1016/j.csite.2021.101687.

16. Selvaraj K, Natarajan A. Factors influencing the performance and productivity of solar stills-A review. Desalination. 2018;435:181-7. http://doi.org/10.1016/j.desal.2017.09.031.
17. Attia MEH, Abdelgaied M, Abdel-Aziz MM, Bellila A, Abdullah A. Optimal size of black gravel as energy storage materials for performance improvement of hemispherical distillers. J Energy Storage. 2021;43:103196. http://doi.org/10.1016/j.est.2021.103196.
18. Li Q, Zhao X, Li L, Hu T, Yang Y, Zhang J. Facile preparation of polydimethylsiloxane/carbon nanotubes modified melamine solar evaporators for efficient steam generation and desalination. J Colloid Interface Sci. 2021;584:602-9. http://doi.org/10.1016/j.jcis.2020.10.002. PMid:33160185.
19. Zhang C, Chen Z, Xia Z, Waldman RZ, Wu S L, Yang HC, Darling SB. Ferric tannate photothermal material for efficient water distillation. Environ Sci.: Water Res Technol. 2020;6(4):911-5. http://doi.org/10.1039/C9EW01016E.
20. Rajan AS, Raja Marimuthu P. Increasing the productivity of pyramid solar still augmented with biomass heat source and analytical validation using RSM. Desalination Water Treat. 2016;5710(10):4406-19. http://doi.org/10.1080/19443994.2014.995133.
21. Dias JF, Toffoli SM, Agopyan V. Absorption of red ceramic tiles. In: Brazilian Congress of Ceramics; 2004 May 23–26; São Pedro, SP, Brazil. Proceedings. São Paulo: Brazilian Ceramic Society; 2004. p. 5–64..
22. Castro APDAS. Thermal performance of glass used in civil construction: study in test cells. Campinas: Faculty of Civil Engineering, Architecture and Urbanism, UNICAMP; 2006.
23. Ramos RO, Lima CAP, Calvacante GG, Medeiros KM. Innovation Privilege. Integrated multianalysis system with connectivity and datalogger function for monitoring solar desalination plants and other water and effluent treatment systems. Brazil patent BR1020210075996, 2021, Apr. 21.
24. Chua HT, Rahimi B. Low grade heat driven multi-effect distillation and desalination. Cham: Elsevier; 2017.
25. El-Agouz SA, El-Samadony YAF, Kabeel AE. Performance evaluation of a continuous flow inclined solar still desalination system. Energy Convers Manage. 2015;101:606-15. http://doi.org/10.1016/j.enconman.2015.05.069.
26. Cardoso MKB, da Silva KS, Silva CB, de Lima GGC, de Medeiros KM, de Lima CAP. Low-cost solar still with corrugated absorber basin for water desalination. J Braz Soc Mech Sci Eng. 2022;44(5):214. http://doi.org/10.1007/s40430-022-03520-z.
27. El-Sebaii AA, Al-Ghamdi AA, Al-Hazmi FS, Faidah AS. Thermal performance of a single basin solar still with PCM as a storage medium. Appl Energy. 2009;86(7-8):1187-95. http://doi.org/10.1016/j.apenergy.2008.10.014.
28. Dunkle RV. Solar water distillation, the roof type solar still and a multi effect diffusion still. In: International Developments in Heat Transfer. ASME Proceedings of International Heat Transfer; 1961; USA. Proceedings. Boulder, CO: University of Colorado; 1961. Pt 5, p. 895-902.
29. Dumka P, Mishra DR. Performance evaluation of single slope solar still augmented with the ultrasonic fogger. Energy. 2020;190:116398. http://doi.org/10.1016/j.energy.2019.116398.
30. Silva KS, de Brito YJV, Silva CB, de Lima GGC, Medeiros KM, Lima CAP. Study of solar still in 565 groundwater treatment in Brazilian northeast. Desalination Water Treat. 2023;293:566. http://doi.org/10.5004/dwt.2023.29550.
31. Baird RB, Eaton AD, Rice EW. Standard methods for the examination of water and wastewater. 23rd ed. Washington, D.C.: American Public Health Association; 2017. 1496 p.
32. Patel P, Kumar R. Comparative performance evaluation of modified passive solar still using sensible heat storage material and increased frontal height. Procedia Technology. 2016;23:431-8. http://doi.org/10.1016/j.protcy.2016.03.047.
33. Priya SS, Mahadi UI. Effect of different absorbing materials on solar Manipal. Ijaiem. 2013;2:301-4.
34. Conserva VR, Silva CB, Ramirez RC, Silva KS, Medeiros KM, Lima CAP. Influence of the wind generator and thermal electrical modules in the solar still in the continuous production of fresh water. ACS ESeT Water. 2024;4(11):5039-52. http://doi.org/10.1021/acsestwater.4c00636.
35. Khechekhouche A, Haoua BB, Kabeel AE, El Hadi Attia M, El-Maghlany WM. Improvement of solar distiller productivity by a black metallic plate of zinc as a thermal storage material. J Test Eval. 2021;49(2):967-76. http://doi.org/10.1520/JTE20190119.
36. Incropera F. Heat and mass transfer. Chicago: GEN|National Editorial Group; 2003.
37. Ravichandran L, Rusovs D, Arjunan TV, Vijayan S, Matheswaran M. Experimental study of brackish water distillation in single slope solar still using sensible heat storage materials. In 8th International Scientific Conference "Rural Development"; 2017; India. Proceedings. Lithuania: Aleksandras Stulginskis University; 2017. p. 391-6. http://doi.org/10.15544/RD.2017.086.
38. Silva CB, da Silva KS, Sarmento KKF, Andrade PS, Cavalcante GG, Medeiros KM, et al. Removal of the veterinary antibiotics oxitetracycline from contaminated water by solar distillation. J Water Process Eng. 2024;58:104784. http://doi.org/10.1016/j.jwpe.2024.104784.
39. Tabrizi FF, Dashtban M, Moghaddam H. Experimental investigation of a weirtype cascade solar still with built-in latent heat thermal energy storage system. Desalination. 2010;260(1-3):248-53. http://doi.org/10.1016/j.desal.2010.03.033.
40. Hailu BT, Fekadu M, Nauss T. Availability of global and national scale land cover products and their accuracy in mountainous areas of Ethiopia: a review. J Appl Remote Sens. 2018;12(4):041502-041502. http://doi.org/10.1117/1.JRS.12.041502.
41. Samuel DH, Nagarajan PK, Sathyamurthy R, El-Agouz SA, Kannan E. Improving the yield of fresh water in conventional solar still using low cost energy storage material. Energy Convers Manage. 2016;112:125-34. http://doi.org/10.1016/j.enconman.2015.12.074.
42. Kabeel AE, El-Agouz SA, Sathyamurthy R, Arunkumar T. Augmenting the productivity of solar still using jute cloth knitted with sand heat energy storage. Desalination. 2018;443:122-9. http://doi.org/10.1016/j.desal.2018.05.026.
43. Benatiallah A, Kalloum S, Benatiallah D. Experimental study of solar still using local material in south of Algeria. AIP Conf Proc. 2018;1968:030024. http://doi.org/10.1063/1.5039211.
44. Kabeel AE, Abdelgaied M, Eisa A. Enhancing the performance of single basin solar still using high thermal conductivity sensible storage materials. J Clean Prod. 2018;183:20-5. http://doi.org/10.1016/j.jclepro.2018.02.144.
45. Balaji R, Udhayakumar CSK, Vijay DA. Performance analysis of solar still using sensible heat storage. Int J Innov Res Adv Eng. 2019;6:1-11. http://doi.org/10.1016/j.rser.2022.112085.
46. Panchal H, Patel DK, Patel P.Theoretical and experimental performance analysis of sandstones and marble pieces as thermal energy storage materials inside solar still. Int J Ambient Energy. 2017;39(3):221-9. http://doi.org/10.1080/01430750.2017.1298059.
47. Arunkumar T, Wang J, Rufuss DDW, Denkenberger D, Kabeel AE. Sensible desalting: investigation of sensible thermal storage materials in solar stills. J Energy Storage. 2020;32:101824. http://doi.org/10.1016/j.est.2020.101824.
48. Li G. Sensible heat thermal storage energy and exergy performance evaluations. Renew Sustain Energy Rev. 2016;53:897-923. http://doi.org/10.1016/j.rser.2015.09.006.
49. WHO: World Health Organization. Guidelines for drinking-water quality: fourth edition incorporating the first addendum 2017. Geneva: WHO; 2017.

50. Cardoso MKB, Brito YJV, Silva KS, Silva CB, Lima CAP, Medeiros KM. Dessalinizador solar do tipo cascata aplicado em poços artesianos no interior da Paraíba. Águas Subterr. 2020;34(2):135-42. http://doi.org/10.14295/ras.v34i2.29799.
51. Tosic M, Restrepo JD, Lonin S, Izquierdo A, Martins F. Water and sediment quality in Cartagena Bay, Colombia: seasonal variability and potential impacts of pollution. Estuar Coast Shelf Sci. 2019;216:187-203. http://doi.org/10.1016/j.ecss.2017.08.013.

Data Availability

Data will be made available on request.